

AN EVALUATION OF SENSOR-PLACEMENT-AGNOSTIC SONOMYOGRAPHY FOR CONTINUOUS CONTROL BY USERS WITH HETEROGENOUS CAPABILITIES

Gavin Suelztz[†], Vikram Athithan^{*1}, Emma Ferran^{*1}, Maria Herrera^{*1}, Carson J. Wynn^{*1}, and Laura A. Hallock¹

^{*}Equal Contribution

¹University of Utah

[†]gavin.suelztz@utah.edu

Introduction: Every cervical spinal cord injury (SCI) is unique: most injuries are incomplete [1], and survivors exhibit heterogeneous neuromotor capabilities. Commercially available interfaces for assistive devices are generally designed assuming either no volitional control below the neck (e.g., sip-and-puff [2]) or capability to drive a joystick [3,4,5], failing to take advantage of other muscle activations users are capable of providing. Sonomyography (SMG) is a promising alternative interface in which exertion-associated tissue motions are processed into continuous or discrete signals. Previous work showed that SMG can be used for continuous proportional control of assistive devices like prostheses [6], but existing methods require large data sets [6] and/or manual feature selection [7,8], preventing use in new contexts without prohibitively time-intensive calibration. Instead, we utilize automated feature detection [9] and sparse optical flow [10] to develop a novel low-training-data, sensor-placement-agnostic SMG control interface. We evaluate performance of this interface in SCI survivors and uninjured users across sensor placements spanning the arm, neck, and upper torso.

Methods²: Our SMG interface consists of a B-mode ultrasound probe placed on an arbitrary body location at which the user can generate visible tissue motion (Figure 1). Users are asked to define a “neutral” pose, followed by poses corresponding to “up” and “down” extrema of an on-screen cursor, while automatically extracted image features [9] are tracked using iterative Lucas–Kanade optical flow estimation [10]. These poses are then used to define a normalized axis of variation for each tracked point, and the user’s cursor position is calculated as the mean of all point locations on their respective axes.

We evaluated the performance of this interface in a pilot cohort of 3 cervical SCI survivors (3 male, age 38 ± 18.4 y) and 6 uninjured individuals (3 male and 3 female, age 29.2 ± 14.2 y). Each participant attempted a control task at the 6 sensor placements listed in Figure 2 up to 2 times each for 2 distinct pose mappings (one prescribed and one self-selected). Following each trial’s pose calibration, users were first allowed unbounded time to practice, then instructed to perform a 2 min trajectory tracking task, shown in Figure 2 (top), following a target circle (Figure 1(a)). Users’ subjective impressions of the system were collected through Likert-style and free form survey questions following each placement. Performance was quantified as root mean squared error (RMSE) between target and user-generated trajectories, normalized to screen height.

Results & Discussion: All participants achieved continuous control at all tested sensor locations. RMSE between SCI survivors and uninjured participants does not illuminate any differences between the two cohorts. Notably, even when the probe was placed across muscles for which the user had no volitional control, if they could identify motions generating sufficient tissue deformation (e.g., leveraging residual antagonist function), these sensor placements could still be used. A good example is one SCI survivor participant who reported no flexor function and was unable to execute the prescribed wrist flexion/extension motion, but was able to use the FLE sensor placement via a forearm supination/pronation mapping as seen in Figure 2 (top). Figure 2 (bottom) shows the RMSE across all participants for each sensor placement, stratified across trajectory segments. The 6 sensor placements all performed similarly across each segment of the trajectory, highlighting the placement-agnostic nature of this algorithm. The exemplar trajectory in Figure 2 (top) illustrates the underlying source of this steadily increasing error, as overshoot and lag in reaction time happens more often due to more frequent direction changes and users more often visit their workspace extrema, where performance degrades. The best-performing placements were able to achieve $\approx 10\%$ error on average during even the final segment’s challenging, highly dynamic task, illustrating system responsiveness.

When asked to rank sensor placements, users’ preferences were heterogeneous. Many communicated prioritizing intuitive control, minimal fatigue, and, for those with SCI, control schemes that did not interfere with trunk balance. Participants highlighted control schemes for which motions of the body and the on-screen cursor were kinematically similar as particularly easy to control.

Significance: Users’ strong tracking performance and positive system impressions demonstrate SMG’s promise for sensor-placement-agnostic device control, while heterogeneous performance and preferences across placements reinforce the need for such interfaces. The developed algorithms have been open-sourced to support further development by scientific and user communities.

Acknowledgments: The authors acknowledge the contributions of Aaron and Amanda Collyer, Denise Gregg, Jennifer Molnar, Ari Sanders, Gabe Parra, and Ajay Anand.

References: [1] B. Sheldon et al. (2025) *World Neurosurgery*. [2] I. Mougharbel et al. (2013) *Science and Information Conference*. [3] G.I. Henderson et al. (2013) *Technology and Disability*. [4] I. Rulik et al. (2022) *Frontiers in Robotics and AI*. [5] S. Aspelund et al. (2020) *PLOS One*. [6] A. Dhawan et al. (2019) *Scientific Reports*. [7] L.A. Hallock et al. (2020) *BioRob*. [8] L.A. Hallock et al. (2021) *TNSRE*. [9] J. Shi and C. Tomasi (1994) *CVPR*. [10] B.D. Lucas and T. Kanade (1981) *IJW*.

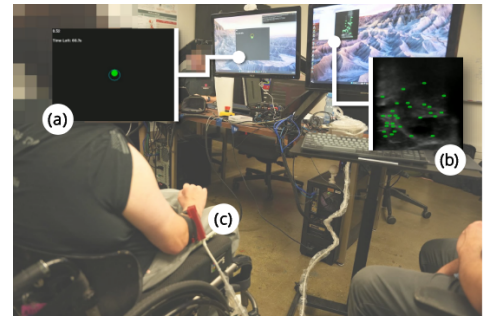


Figure 1: Optical-flow-based sonomyography (SMG) control method enabling users to control the vertical position of on-screen cursor (a) using SMG data (b) from probe (c) placed on arbitrary body locations after minimal calibration (3 pose definitions).

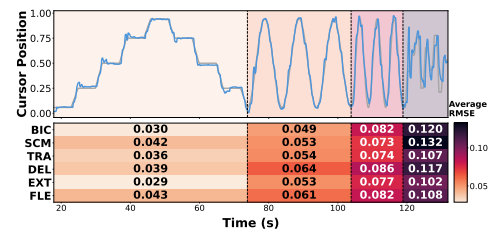


Figure 2: Top: Exemplar target (gray) and user-generated (blue) trajectories illustrate the primary underlying sources of error (SCI participant, placement FLE). Bottom: Average RMSE for each sensor placement during each trajectory segment. Muscle placements corresponding to the reported values are (in order): biceps, sternocleidomastoid, trapezius, deltoid, wrist extensors, and wrist flexors.

²Approved under University of Utah IRB Protocol IRB_00183389.